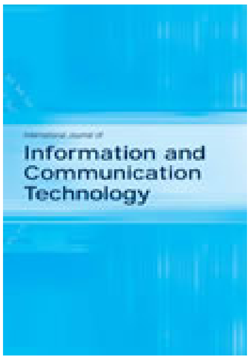

International Journal of Information and Communication Technology

ISSN online: 1741-8070 - ISSN print: 1466-6642
https://www.inderscience.com/ijict

College student management based on machine vision and intelligent monitoring system

Yawei Han

Article History:

Received:	15 September 2023
Last revised:	27 October 2023
Accepted:	13 November 2023
Published online:	05 March 2024

College student management based on machine vision and intelligent monitoring system

Yawei Han

Marxism Institute,
Sichuan University,
Chengdu Sichuan, 610065, China
Email: 15922964886@163.com

Abstract: This paper combines machine vision and intelligent detection technology to construct a college student management system. In student feature recognition, this paper uses the frustum plane calculation formula to determine the range of the current viewpoint, and then encloses the grid nodes in the form of spherical bounding boxes to eliminate invalid nodes to simplify the loading and rendering of invalid nodes. This article uses the Bresenham algorithm for rasterising vector lines. Then, this paper proposes a dual node evaluation system based on viewpoint distance and node area complexity to refine the nodes. At the same time, this paper adopts an adaptive method to select the repair of cracks. The effectiveness of the method proposed in this paper has been verified through numerical comparative experiments.

Keywords: machine vision; intelligent monitoring; college students; management.

Reference to this paper should be made as follows: Han, Y. (2024) 'College student management based on machine vision and intelligent monitoring system', *Int. J. Information and Communication Technology*, Vol. 24, No. 2, pp.228–244.

Biographical notes: Yawei Han graduated from the Lanzhou University of Management Institute in 2014. He studied in Marxism Institute, Sichuan University. His research interests include Sinicization of Marxism and student education.

1 Introduction

With the advent of economic globalisation and information networking, the communication between people and the exchange of information transcends any geographical, time, and object restrictions. Moreover, the scope of communication is all over the world, and the speed of communication is shortened to an instant. (Lauguico et al., 2020).

At present, the management of college students is based on the guiding ideology to meet the stability and development of the school, and focus on cultivating students to meet the requirements of predetermined goals. (Benbarrad et al., 2021); The formation of meaning levels such as the value pursuit and moral experience of college teachers and students needs to be ignored to varying degrees (Zhang et al., 2020). The people trained by education and management are not complete people, and they are not in accordance with the essence of people. 'In a comprehensive way, that is, Said, as a whole person, possessing one's full essence' (Li et al., 2020).

In management activities, teachers are the party with dominant resources and have the initiative; while college students are often in a passive and disadvantaged position, losing their due thought and right to speak. Lost the attribute of 'freedom' (Elaskari et al., 2021). As the receiving subject of education management, the freedom, initiative, and creativity that the 'subject' should have disappeared (Eguiraun et al., 2018).

The daily life of college students is not an ordinary life, but a special life, a noble, rich and meaningful life with 'education' as the core connotation, we might as well call it 'educational life'. In the current management of college students, there has been a long-term education management that equates publicity, implementation of rules and regulations, and setting an example with students, forgetting the rich teacher-student relationship, ignoring the communication, dialogue, experience, and understanding between teachers and students, and forgetting the right relationship between teachers and students. The improvement of students' humanity (Goldberg et al., 2021). In fact, the function of teachers is not only to impart knowledge, but to create more communication between teachers and students, so that students can experience equality, democracy, respect and understanding in the interaction between teachers and students, and form this educational teacher-student relationship (Li et al., 2021). The process of teachers imposing knowledge on students from the outside to the inside, ignoring that the educational process is actually an on-the-spot experience (Ngoc Anh et al., 2019).

Create teacher-student interaction in many places, so that students can experience equality, democracy, respect and understanding in teacher-student interaction (Zhu et al., 2019). Teachers are accustomed to instilling the profound moral goals and abstract moral content in books as a kind of moral concept, and these concepts are far from the behaviour in real life. College students can only recite these abstract and empty moral normative knowledge, but they cannot experience the richness and freshness of the real life world, and still go their own way in real life (Palconit et al., 2021). The so-called strict management. In fact, it is necessary to have an advanced management concept, a set of reasonable management systems, and correct implementation strategies (Gummineni, 2020). Many predecessors have defined strict management, from the original meaning. Strict management is to follow the educational goals and educational laws and the laws of management activities themselves, and adopt scientific methods and measures (Liu et al., 2021).

Applying management theory to the management of college students, the management department should first clarify its own responsibilities, scientifically divide the student management work, and divide different students into different managers under the guidance of the contracting system to ensure that each Managers can consciously assume their own responsibilities and effectively improve the efficiency and effectiveness of management work (Kariapper, 2021). Colleges and universities should realise that student management is not only an important task that every administrator should shoulder, but also has a close relationship with ordinary teachers (Guo et al., 2020). In order to ensure the effect of student management, college administrators should pay attention to regularly adjusting and summarising the management plan in the management process, to ensure that problems existing in student management can be discovered and solved in time, and the effect of college student management can be maximised. highlighted (Lin et al., 2020).

The advantages of this article are as follows:

In order to reduce the rendering pressure of the system and improve its smoothness, a clipping method based on spherical bounding boxes for view cones is proposed, which removes nodes outside the view range and reduces the loading of grid nodes.

A dual node evaluation system has been established to address issues such as cracks and faults that occur during data rendering. The current node subdivision level is calculated based on viewpoint distance and node region complexity, and a nonlinear decreasing mutation operator is introduced to adaptively select methods to eliminate cracks

The system constructed in this article has certain value in strengthening school safety management and enhancing the school's ability to respond to emergencies. With the construction and deployment of the system, a security management information network covering the entire campus will be established, establishing a three-level efficient information management model for managers, teachers, and students. This move will leverage the security management and education functions of this system, while fully applying modern information management technology to the school security management platform, opening a new page in the field of school security management.

This paper combines machine vision and intelligent detection technology to construct an intelligent management system for college students to improve the effect of modern college students' management.

2 Intelligent detection based on machine vision

It also laid a solid foundation for the expansion of system functions and related applications in the future. The system combines the above technical means with school safety management work, and cooperates with school safety management activities and events of different needs to achieve data collection, sharing, and analysis of student situations. This enables various departments of the school to handle and prevent various safety incidents and applications reported by students and management personnel in a timely and effective manner. The staff of the school safety administrative department can timely understand student safety dynamics, school safety incidents, and other work through multimedia forms such as text and pictures. This system has certain value in strengthening school safety management and enhancing the school's ability to respond to emergencies

2.1 Rasterisation of vector data

Before the vector data is rasterised, the division standard of the raster matrix needs to be determined first. After the vector data is rasterised, the geometric accuracy of the image will be reduced to a certain extent. Therefore, in the determination of the grid size standard, the accuracy of the image should be ensured as much as possible, so that the low accuracy and aliasing of the image edges will not occur when the grid data is rendered later. At the same time, the resolution of the image depends on the degree of subdivision of the pixels. In order to improve the rendering accuracy and ensure the rendering quality of marine data, it is necessary to subdivide the raster data, but the raster data is expressed in the form of squared exponents. Therefore, the determination of the grid matrix is one of the key factors affecting the size of grid data. Therefore, before the vector data is rasterised, it is necessary to clarify the division standard of the raster matrix. The representation of the grid matrix is shown in Figure 1. $\Delta X * \Delta Y$ is the size of a grid cell, and (X_0, Y_0) is the coordinate origin of the grid data.

Figure 1 Grid matrix (see online version for colours)

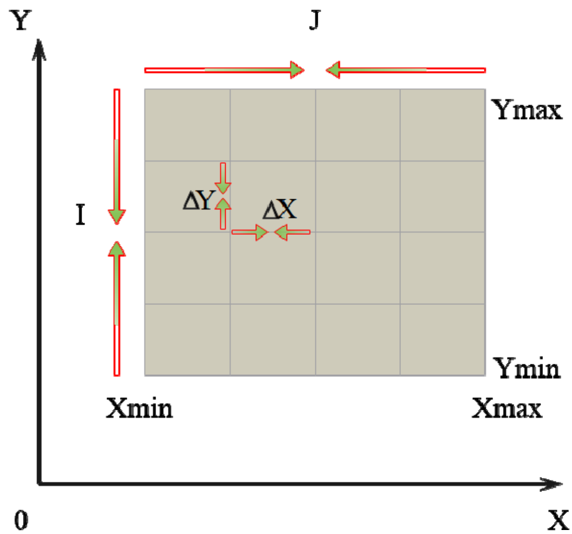

Among them, the calculation formulas of *I* and *J* are shown in 1 and 2:

$$I = \frac{(Y_{\max} - Y_{\min})}{\Delta X} \tag{1}$$

$$J = \frac{(X_{\max} - X_{\min})}{\Delta Y} \tag{2}$$

In the formula, *I* and *J* represent the row and column numbers of the raster data cells, ΔX and ΔY represent the width and height of a grid respectively, X_{max} and X_{min} represent the maximum and minimum values of the X-axis, respectively, and Y_{max} and Y_{min} represent the maximum and minimum values of the Y-axis, respectively.

Simply put, the rasterisation of points is to convert the coordinate values of the vector points into the row and column values *I*, *J* corresponding to the grid matrix, and then represent the specific position of the point in the form of row and column numbers, as shown in Figure 2:

Among them, the conversion of points is shown in equation (3) and (4):

$$I = 1 + INT\left[\frac{Y_{\max} - Y}{\Delta X}\right] \tag{3}$$

$$J = 1 + INT\left[\frac{X_{\max} - X}{\Delta Y}\right] \tag{4}$$

In the formula, *INT*[] indicates that the operation result is rounded to ensure that the values of *I* and *J* are positive.

Figure 2 Rasterisation of points (see online version for colours)

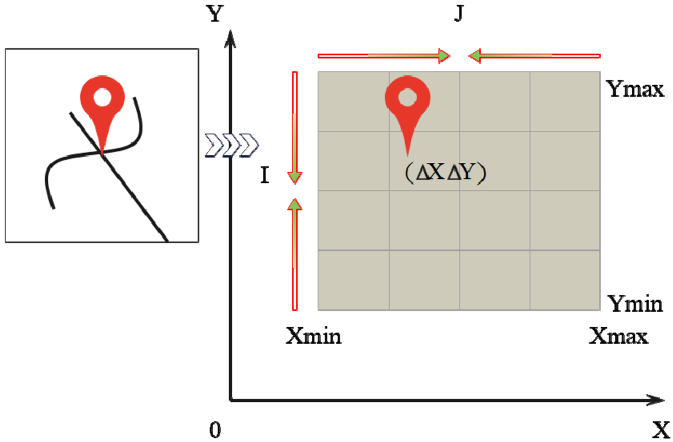

The operation principle of the DDA algorithm is shown in Figure 3:

Figure 3 DDA algorithm (see online version for colours)

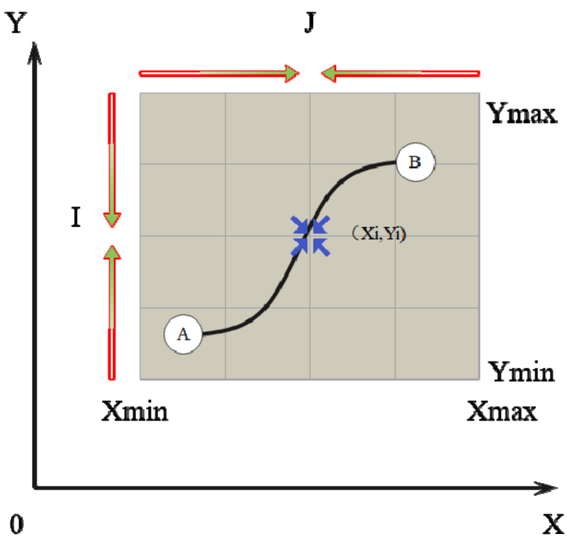

We set the intersection of (X_A, Y_A), (X_B, X_B) and the grid as (X_i, Y_i), then there is:

$$X_{i+1} = X_i + \frac{X_B - X_A}{n} = X_i + \Delta X \tag{5}$$

$$Y_{i+1} = Y_i + \frac{Y_B - Y_A}{n} = Y_i + \Delta Y \tag{6}$$

Among them, there is $n = max(|X_B – X_A|, |Y_B, Y_A|)/d$ $\Delta X = (X_B – X_A)/n$, and $\Delta Y = (Y_B – Y_A)/n$. When there is $i = 0$, there is $X_0 = X_A$ and $Y_0 = Y_A$. When $i = n–1$ is calculated, there is $X_n = X_B$. By calculating from $i = 0$ to $i = n–1$, several intersection coordinates of the vector line segment and the grid can be obtained. After rounding it, the raster data of the entire line segment can be obtained.

In this paper, Bresenham algorithm is used to rasterise vector lines.

Figure 4 Bresenham's algorithm (see online version for colours)

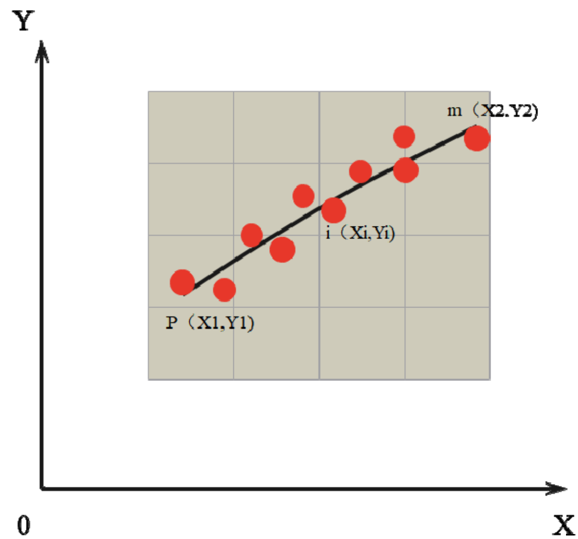

As shown in Figure 4, it is assumed that point $p(x_1, y_1)$ is the start point of the vector line, and $m(x_2, y_2)$ is the end point of the line. It is shown in equations (7)–(9) according to the slope of the straight line

$$k = \frac{\Delta Y}{\Delta X} \tag{7}$$

$$\Delta x = x_2 - x_1 \tag{8}$$

$$\Delta y = y_2 - y_1 \tag{9}$$

The equation of the line is set to $y = kx + b$, the coordinate of the i^{th} data point on the line is (X_i, Y_i), and the approximate data point coordinate of this point is (x_i, y_i). When there is $x_i = X_i$, the coordinates of the next point may be $(x_i + 1, y_i + 1)$ or $(x_i + 1, y_i)$. The distance d between the coordinate point and the line point is calculated as shown in equations (10)–(12).

$$y = k(x_i + 1) + b \tag{10}$$

$$d_1 = y - y_i \tag{11}$$

$$d_2 = (y_i + 1) - y \tag{12}$$

In the formula, d_1 and d_2 are the distance between the abscissa and the ordinate of the line point, respectively. The distance difference Δd of the two distances is calculated according to equation (13).

$$\Delta d = d_1 - d_2 = 2k(x_i + 1) - 2y_i + 2b - 1 \tag{13}$$

It can be seen from this that the selection of the approximate coordinate point of the next point of the line is mainly determined by Δd. Therefore, in order to make the calculation of Δd simpler, the calculation formula of Δd will be re-determined below, as shown in equation (14).

$$\begin{aligned} H_i &= \Delta x * \Delta d \\ &= \Delta x * \left[2k(x_i+1) - 2y_i + 2b - 1\right] \\ &= 2k\Delta x(x_i+1) - 2\Delta x y_i + \Delta x(2b-1) \end{aligned} \tag{14}$$

In the formula, there is $\Delta x > 0$, so it can be deduced that $H_i > 0$. A constant variable e is used to further simplify the formula to obtain:

$$H_i = 2\Delta y x_i - 2\Delta x y_i + [2\Delta y + \Delta x(2b-1)] \tag{15}$$

$$e = 2\Delta y + \Delta x(2b-1) \tag{16}$$

Therefore, there are:

$$H_i = 2\Delta y x_i - 2\Delta x y_i + e \tag{17}$$

By simplifying the calculation of H_i, the next approximate result of H_{i+1} can be obtained, as shown in equation (18):

$$\begin{aligned} H_{i+1} &= 2\Delta y x_{i+1} - 2\Delta x y_{i+1} + e \\ &= 2\Delta y\left(x_i+1\right) - 2\Delta x y_{i+1} + e \\ &= \left(2\Delta y x_i - 2\Delta x y_i + e\right) + 2\Delta y + 2\Delta x y_i - -2\Delta x y_{i+1} \\ &= H_i + 2\Delta y - 2\Delta x\left(y_{i+1} - y_i\right) \end{aligned} \tag{18}$$

Among them, the calculation of variable H_{i+1} is only related to H_i. Therefore, in order to obtain the coordinate position of each point, the initial value of needs to be calculated, and its calculation formula is shown in 19:

$$\begin{cases} p_1 = 2\Delta y x_1 - 2\Delta x y_1 + e \\ y_1 = kx_1 + b \\ k = \dfrac{\Delta y}{\Delta x} \\ e = 2\Delta y + \Delta x(2b) - 1 \end{cases} \tag{19}$$

The system of equations are combined and solved:

$$p_1 = 2\Delta y - \Delta x \tag{20}$$

To sum up, the Bresenham algorithm uses the discriminant variable to represent the coordinate position of the next point, as shown in equation (21)

$$\left(x_{i+1}, y_{i+1}\right) = \begin{cases} \left(x_i+1, y_i+1\right), H_{i+1} = +2(\Delta y - \Delta x)\left(H_i \geq 0\right) \\ \left(x_i+1, y_i\right), H_{i+1} = H_i + 2\Delta y\left(H_i < 0\right) \end{cases} \tag{21}$$

Figure 5 Ray algorithm (see online version for colours)

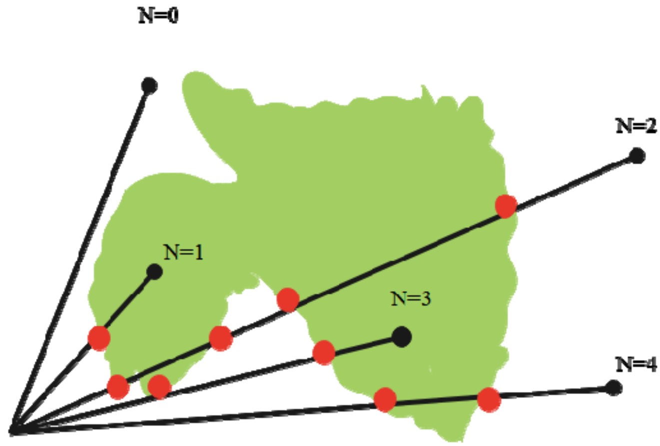

As shown in Figure 5, there are 5 rays in total, which respectively represent 5 points to be detected. When there is N = 1, it means that the induced line has an intersection point with the vector polygon, which means that the point to be measured is located in the local part of the polygon. When the number of intersection points is N = 2, it means that the induced line and the vector polygon have two intersection points, which means that the point to be measured is located outside the polygon. The rest of the situation is analogous, and will not be repeated here. However, after research, it is found that the ray algorithm also has some problems to a certain extent, such as the existence of ambiguous points, as shown in Figure 6.

Figure 6 Ambiguity point

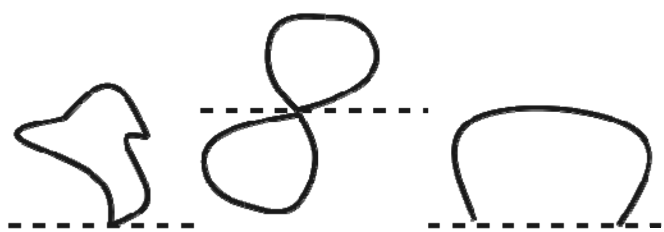

The improvement of the scanning ray algorithm is essentially to improve the ray extraction direction on the basis of the ray algorithm, so that it emits scan lines along the row direction (horizontal ray) or the column direction (vertical ray) of the grid matrix.

As shown in Figure 7, for a given polygonal graph, several parallel scan lines are used to scan in a top-down order, and each scan line has an intersection point with the polygonal graph. These intersection points divide the scan line into two parts, one part of the line segment is inside the polygon, and the other part of the intersection point is outside the polygon, and the whole is arranged alternately.

Figure 7 Improved ray scanning algorithm (see online version for colours)

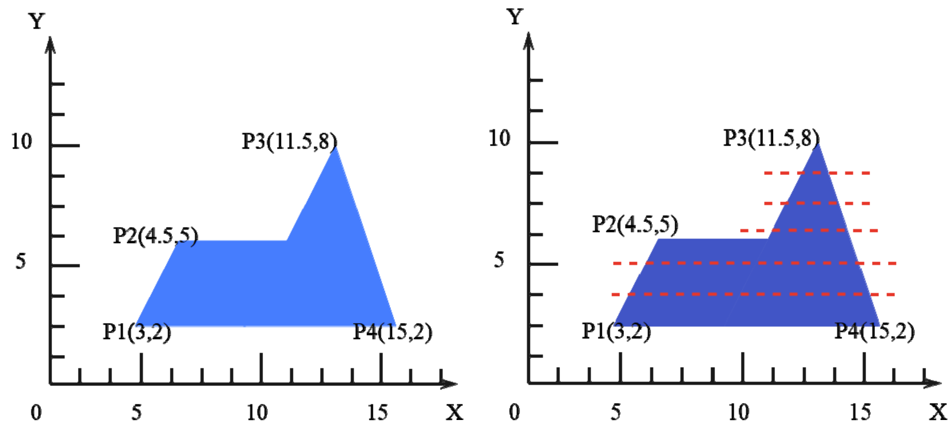

2.2 The principle of the frustum

The frustum can be simply viewed as the distance between the user's viewpoint and the screen. It responds in real-time according to the change of the user's viewpoint range, so as to decide which grid nodes need to be loaded, rendered, and which nodes need to be eliminated. The frustum structure is shown in Figure 8.

Figure 8 Frustum imaging (see online version for colours)

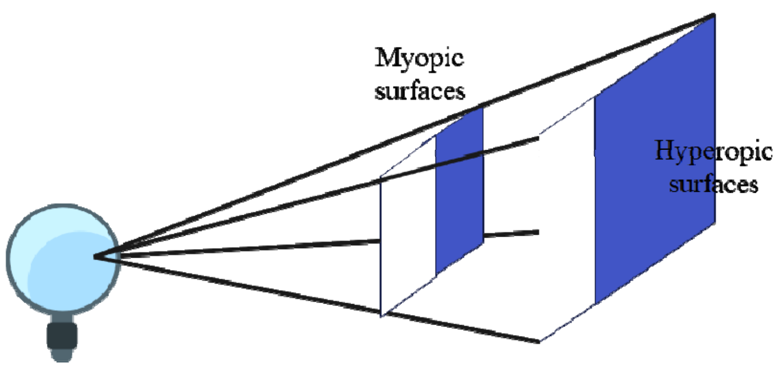

The viewing cone is divided into six planes, which are composed of the upper plane, the lower plane, the left plane, the right plane, the near-sighted plane and the far-sighted plane. If the viewpoint is outside the view frustum, it needs to be clipped by the viewpoint culling algorithm. If the viewpoint is inside the frustum, the data in the range of the viewpoint will be rendered. As shown in Figure 9, the green in Figure 9(a) represents the number of rendering meshes currently required, the red triangle area represents the range size of the current viewpoint, and Figure 9(b) represents the number of rendering meshes required after viewpoint culling. It can be seen that after viewpoint culling, the number of corresponding mesh renderings is significantly reduced.

Figure 9 Viewpoint culling, (a) before the node is removed (b) after the node is removed (see online version for colours)

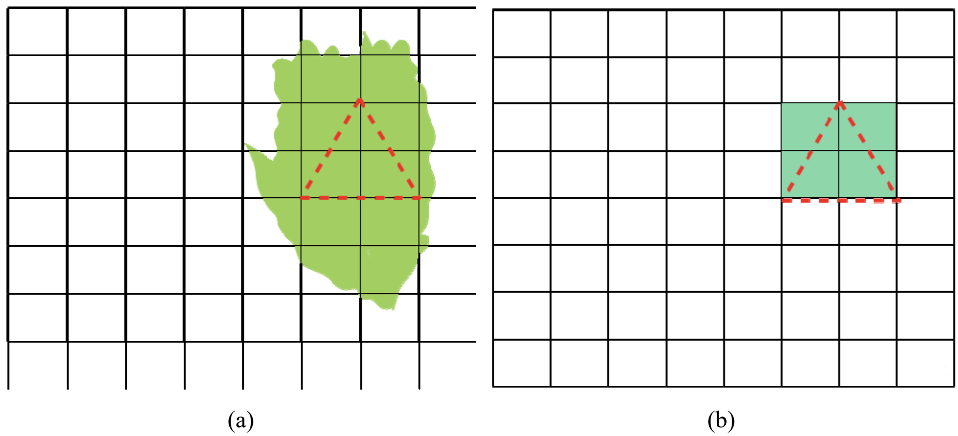

2.3 Viewpoint culling method

In order to determine the range of the viewpoint more accurately, it is necessary to derive the space plane equations of the six faces of the viewing cone. The near plane is used as an example. First, the view frustum plane equation can be expressed as $A_x + B_y + C_z + D = 0$. Second, a point $p = (X, Y, Z, W)$ in the near plane and a 4 * 4 projection matrix $M = m(i, j)$ are defined. Then, the matrix M is used to transform the point p, and the transformed vertex is $p' = (X', Y', Z', W)$, which can be written as the following formula:

$$pM = \begin{bmatrix} p * row_0 \\ p * row_1 \\ p * row_2 \\ p * row_3 \end{bmatrix} = [X, Y, Z, W] \begin{bmatrix} m_{00} & m_{01} & m_{02} & m_{03} \\ m_{10} & m_{11} & m_{12} & m_{13} \\ m_{20} & m_{21} & m_{22} & m_{23} \\ m_{30} & m_{31} & m_{32} & m_{33} \end{bmatrix} = \begin{bmatrix} X' \\ Y' \\ Z' \\ W' \end{bmatrix} = p' \tag{22}$$

For the transformed p', if it is inside the frustum, then:

$$\begin{cases} -W' < X' < W' \\ -W' < Y' < W' \\ -W' < Z' < W' \end{cases} \tag{23}$$

When we judge whether the point p' is in the near plane of the viewing frustum, we only need to judge whether $-M' < X'$ holds, so we get:

$$\begin{cases} -(p * row_3) < (p * row_1) \\ 0 < (p * row_3) + (p * row_1) \\ 0 < (row_1 + row_3) \end{cases} \tag{24}$$

We get:

$$\begin{cases} A = (m_{00} + m_{30}) \\ B = (m_{01} + m_{31}) \\ C = (m_{02} + m_{32}) \\ A = (m_{03} + m_{33}) \end{cases} \tag{25}$$

Therefore, the equations for deriving the near plane are:

$$X(m_{00} + m_{30}) + Y(m_{01} + m_{31}) + Z(m_{02} + m_{32}) + W(m_{03} + m_{33}) = 0 \tag{26}$$

The final solution is:

$$X(m_{00} + m_{30}) + Y(m_{01} + m_{31}) + Z(m_{02} + m_{32}) + (m_{03} + m_{33}) = 0 \tag{27}$$

In the same way, the expressions of several other planes can be solved, and then the coordinate value of the viewpoint is brought into each expression for judgment. If all six faces satisfy $A_x + B_y + C_z, + D > 0$ it means that the viewpoint is within the viewing frustum. If not, it means that the viewpoint is outside the frustum, and viewpoint culling needs to be performed.

The radius r of the spherical bounding box is equidistant. Therefore, it is only necessary to calculate the distance d between the node and the centre of the sphere, and then compare it with the radius r of the centre of the sphere to determine whether the node is located inside the view frustum, which is more convenient than the hexahedral bounding box (AABB bounding box). A schematic diagram of a spherical bounding box is shown in Figure 10.

Figure 10 Spherical bounding box (see online version for colours)

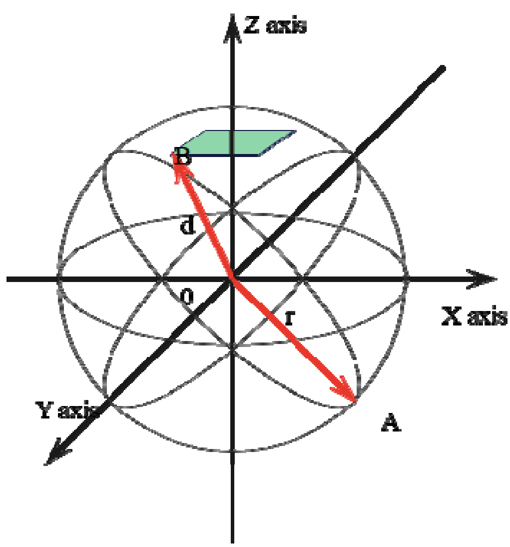

The coordinates of the centre of the spherical bounding box are:

$$(X, Y, Z) = \left(\frac{x_{max} + x_{min}}{2}, \frac{y_{max} + y_{min}}{2}, \frac{z_{max} + z_{min}}{2}\right) \tag{28}$$

In the formula, x_{max}, y_{max}, and z_{max} are the maximum values of the bounding box on the X, Y, and Z axes, respectively, and x_{min}, y_{min}, and z_{min} are the minimum values of the bounding box on the X, Y, and Z axes, respectively. Therefore, the radius r of the bounding box can be expressed as:

$$r = \frac{\sqrt{(x_{\max} - x_{\min})^2 + (y_{\max} - y_{\min})^2 + (z_{\max} - z_{\min})^2}}{2} \tag{29}$$

The distance d from the node to the centre of the sphere can be expressed as:

$$d = \sqrt{(x_{\max} - x_{\min})^2 + (y_{\max} - y_{\min})^2 + (z_{\max} - z_{\min})^2} \tag{30}$$

By calculating the radius of the centre of the bounding box r and the node distance d, the values of r and d are determined.

2.4 Double control factor node evaluation system

Not only are there many types of ocean data, but the data is huge. Excessive data will result in a very low frame rate (FPS) for rendering data, and consume a lot of system resources during the processing of the node. Therefore, in order to enable the system to render marine data without freezing, it is necessary to subdivide and judge the grid nodes through the node evaluation system, so as to realise multi-resolution display of layers. Among them, the control factor node evaluation system is mainly affected by two aspects, one is the user's viewpoint distance, and the other is the node area complexity. Through these two control factors, the data is judged whether it is necessary to continue to divide the nodes.

Figure 11 Viewpoint distance (see online version for colours)

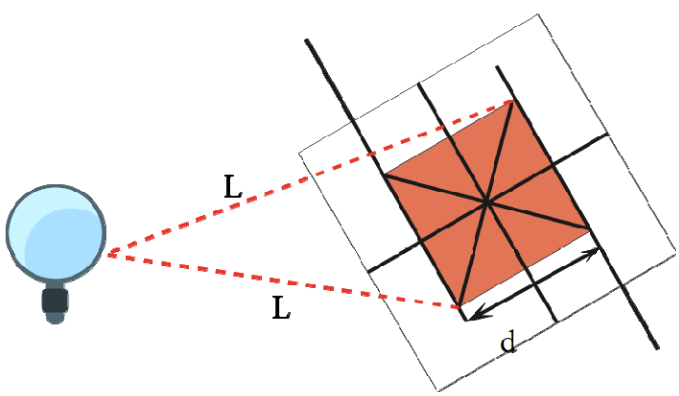

As shown in Figure 11, in the figure, L represents the distance between the grid node and the viewpoint, and d is the side length of the grid node.

Among them, for the calculation of the viewpoint distance L, this paper uses the Manhattan distance calculation formula with small amount of calculation and simple steps to calculate, which can calculate the distance between the viewpoint and the node more accurately, as shown in equation (31):

$$L = |x_1 - x_2| + |y_1 - y_2| + |z_1 - z_2| \tag{31}$$

The control variable that defines the distance between the node and the viewpoint is set to f_1, and the influence of L and node side length d on the degree of node subdivision is controlled by the following formula:

$$f_1 = \frac{L}{d * C_1} \tag{32}$$

In the formula, f_1 represents the control variable of the node sight distance, C_1 is the sight distance control factor, and the influence of the viewpoint distance on the node subdivision degree can be controlled by adjusting the size of C_1. It can be seen from the formula that when C_1 is larger, the value of f_1 is smaller, which indicates that the user's viewpoint is close, so the degree of subdivision of nodes is higher, and the number of polygons drawn is more abundant. When the value of C_1 is small, the value of f_1 is larger, which means that the user's viewpoint is far away at this time, so the degree of subdivision of nodes is low, and only simple drawing is required to render low-resolution rendering.

The degree of subdivision of the data is also closely related to the complexity of the node area. The more complex the node area is, the more times it is divided, which means that the data needs to be rendered in more detail. The node area is shown in Figure 12:

Figure 12 Node area complexity (see online version for colours)

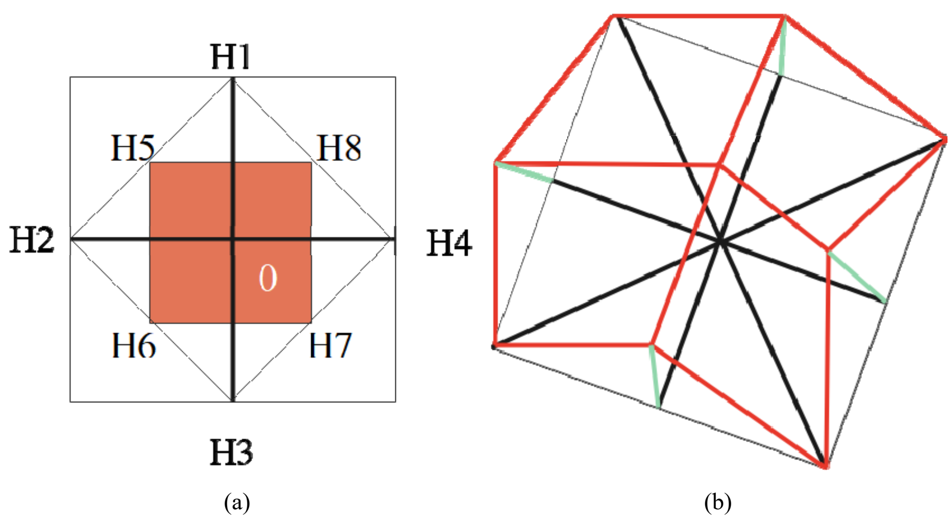

Figure 12(a) shows the eight complexity values of a node. H1–H8 are used to represent the smoothness of the node region. There are a total of eight complexity values, H5–H8 represent the complexity values of the child nodes. Among them, the larger the value, the higher the complexity of the node area. Figure 12(b) represents a schematic diagram of the node area complexity of a quadtree, and the calculation method should satisfy the following formula:

$$f_2 = \frac{L}{r * C_2} \tag{33}$$

In the formula, f_2 represents the control variable of the node area complexity, and C_2 is the node area complexity control factor. When the value of C_2 is larger, the influence on the degree of subdivision is higher, which means that the node area indicated by the data is more complex, and more details need to be presented, so the data needs to be segmented more finely. When the value of C_2 is small, the influence on the degree of subdivision is low, which means that the complexity of the node area is low, the structure is relatively simple, and the degree of subdivision will not be too high.

According to the viewpoint distance control variable f_1 and the node area complexity control variable f_2 of 4.2, this paper integrates two control factors, and proposes a dual control factor node evaluation system based on viewpoint distance and node area complexity. The calculation formula is shown in equation (34):

$$f = \frac{L}{d * r * C_1 * C_2} \tag{34}$$

Among them, when there is $f < 1$, it means that the node needs to continue to be divided. When there is $f \geq 1$, it indicates that the node does not need to be further divided.

3 College student management system based on machine vision and intelligent monitoring system

The college student management system based on machine vision and intelligent monitoring system constructed in this paper is shown in Figure 13.

Figure 13 College student management system based on machine vision and intelligent monitoring system (see online version for colours)

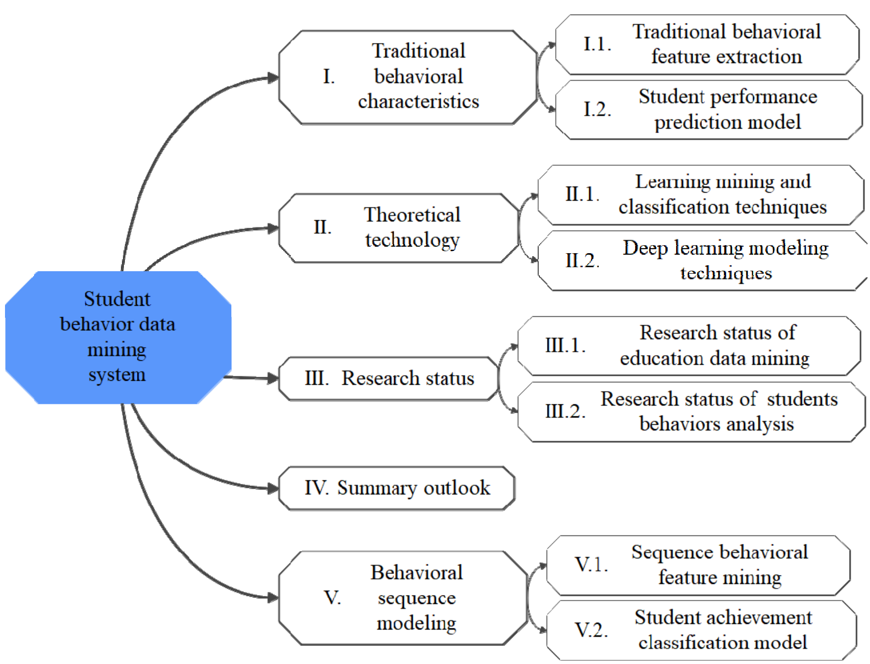

The hardware and software systems for experimental research in this article are shown in Tables 1 and 2.

Table 1 System software environment

Software name	*Device name*
Client operating system	windows10, android/ios
Development environment	NetBeans
server	WampSercer
database	MySQL
Running Platform	Mainstream browsers

Table 2 System software environment

Device name	*Hardware name*
Computer (L APTOP-ML 3C53TN)	CPU(8G + 1T)
Android phone	CPU(8G + 256G)
IOS mobile phone	CPU(8G + 256G)

On the basis of the above, the effect of the college student management system based on machine vision and intelligent monitoring system is verified, and the effect of college student management is studied, and Figure 14 is obtained.

Figure 14 System effect verification (see online version for colours)

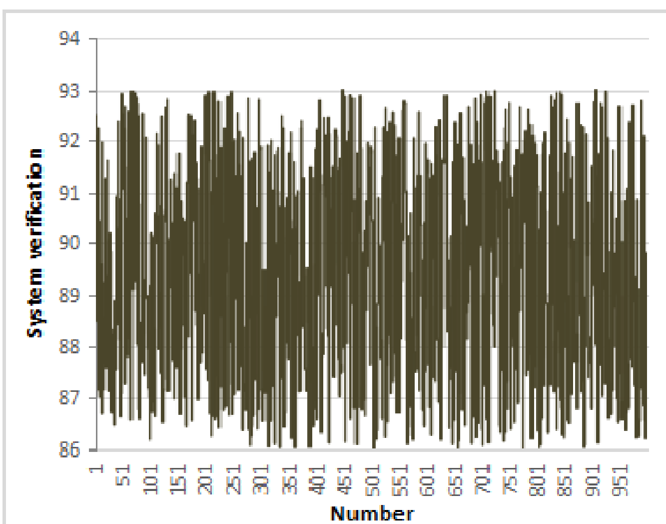

This article utilises the characteristics of student behaviour data to depict students' behaviour, striving to establish a comprehensive understanding of traditional behaviour patterns among students, in order to improve the effectiveness of school management. In terms of algorithm usage, it is not limited to a single algorithm, but rather to selecting multiple algorithms to model student behaviour based on full consideration of data semantic features. The superiority of different algorithms is tested, and the best multi classification prediction model is found. The practicality of this method is verified through experimental research.

From the above results, it can be seen that the college student management system based on machine vision and intelligent monitoring system proposed in this paper can effectively improve the management effect of college students.

The system constructed in this article has certain value in strengthening school safety management and enhancing the school's ability to respond to emergencies. With the construction and deployment of the system, a security management information network covering the entire campus will be established, establishing a three-level efficient information management model for managers, teachers, and students. This move will leverage the security management and education functions of this system, while fully applying modern information management technology to the school security management platform, opening a new page in the field of school security management.

4 Conclusions

At present, there are certain drawbacks in the process of student management in colleges and universities. In the planning, organisation, command, decision-making, control, supervision and other aspects of management, only the figures of managers at all levels of schools, colleges, and departments can be seen, showing their will and ideas. Moreover, they are often self-centred, without students in their hearts, and they care about their superiors and competent departments, and students are only objects and embellishments of execution, thus becoming marginal and outsiders of management. At the same time, management has accordingly become a closed system, and it has become a one-way transmission from school to college, to department, to class, to student leaders, and finally to ordinary students. This paper combines machine vision and intelligent detection technology to construct an intelligent management system for college students to improve the management effect of modern college students. From the test results, it can be seen that the college student management system based on machine vision and intelligent monitoring system proposed in this paper can effectively improve the management effect of college students.

This article utilises the characteristics of student behaviour data to characterise student behaviour. After fully considering the semantic characteristics of the data, multiple algorithms are selected to model student behaviour, and the superiority of different algorithms is tested. The practicality of this method is verified through experimental research.

Although this design has completed the basic envisioned functions, there are still shortcomings that need to be improved in the following areas. Firstly, improvements need to be made to the sensor to make it more sensitive in determining whether the classroom is occupied or not. Finally, improvements need to be made to the upper computer. There are still some shortcomings in the design of the upper computer, and a database should be added to save the collected data.

References

Benbarrad, T., Salhaoui, M., Kenitar, S.B. and Arioua, M. (2021) 'Intelligent machine vision model for defective product inspection based on machine learning', *Journal of Sensor and Actuator Networks*, Vol. 10, No. 1, pp.7–17.

Eguiraun, H., Casquero, O. and Martinez, I. (2018) 'The Shannon entropy trend of a fish system estimated by a machine vision approach seems to reflect the molar Se: Hg ratio of its feed', *Entropy*, Vol. 20, No. 2, pp.90–98.

Elaskari, S., Imran, M., Elaskri, A. and Almasoudi, A. (2021) 'Using barcode to track student attendance and assets in higher education institutions', *Procedia Computer Science*, Vol. 184, No. 1, pp.226–233.

Goldberg, P., Sümer, Ö., Stürmer, K., Wagner, W., Göllner, R., Gerjets, P., ... and Trautwein, U. (2021) 'Attentive or not? Toward a machine learning approach to assessing students' visible engagement in classroom instruction', *Educational Psychology Review*, Vol. 33, No. 1, p.27.

Gummineni, M. (2020) 'Implementing Bloom's taxonomy tool for better learning outcomes of PLC and robotics course', *International Journal of Emerging Technologies in Learning (iJET)*, Vol. 15, No. 5, pp.184–192.

Guo, Z., Zhang, M., Lee, D.J and Simons, T. (2020). 'smart camera for quality inspection and grading of food products', *Electronics*, Vol. 9, No. 3, pp.505–513.

Kariapper, R. K. A. R. (2021). 'Attendance system using RFID, IoT and Machine learning: a two factor verification approach', *Systematic Reviews in Pharmacy*, Vol. 12, No. 3, pp.314–321.

Lauguico, S.C., Concepcion, R.S., Alejandrino, J.D., Tobias, R.R., Macasaet, D.D and Dadios, E.P. (2020) 'A comparative analysis of machine learning algorithms modeled from machine vision-based lettuce growth stage classification in smart aquaponics', *International Journal of Environmental Science and Development*, Vol. 11, No. 9, pp.442–449.

Li, C., Chen, H., Li, X., Xu, N., Hu, Z., Xue, D., ... and Sun, H. (2020) 'A review for cervical histopathology image analysis using machine vision approaches', A*rtificial Intelligence Review*, Vol. 53, No. 7, pp.4821–4862.

Li, H., Zhang, H and Zhao, Y. (2021) 'Design of computer-aided teaching network management system for college physical education', *Computer-Aided Design and Applications*, Vol. 18, No. S4, pp.152–162.

Lin, T.L., Chang, H.Y. and Chen, K.H. (2020) 'The pest and disease identification in the growth of sweet peppers using faster R-CNN and mask R-CNN', *Journal of Internet Technology*, Vol. 21, No. 2, pp.605–614.

Liu, T., Wilczyńska, D., Lipowski, M. and Zhao, Z. (2021) 'Optimization of a sports activity development model using artificial intelligence under new curriculum reform', *International Journal of Environmental Research and Public Health*, Vol. 18, No. 17, pp.9049–9060.

Ngoc Anh, B., Tung Son, N., Truong Lam, P., Phuong Chi, L., Huu Tuan, N., Cong Dat, N., ... and Van Dinh, T. (2019) 'A computer-vision based application for student behavior monitoring in classroom', *Applied Sciences*, Vol. 9, No. 22, pp.4729–4740.

Palconit, M.G.B., Concepcion II, R.S., Alejandrino, J.D., Pareja, M.E., Almero, V.J.D., Bandala, A.A., ... and Naguib, R.N. (2021) 'Three-dimensional stereo vision tracking of multiple free-swimming fish for low frame rate video', *Journal of Advanced Computational Intelligence and Intelligent Informatics*, Vol. 25, No. 5, pp.639–646.

Zhang, S., Yang, X., Wang, Y., Zhao, Z., Liu, J., Liu, Y., ... and Zhou, C. (2020) 'Automatic fish population counting by machine vision and a hybrid deep neural network model', *Animals*, Vol. 10, No. 2, p.364373.

Zhu, S., Feng, L., Zhang, C., Bao, Y and He, Y. (2019) 'Identifying freshness of spinach leaves stored at different temperatures using hyperspectral imaging', *Foods*, Vol. 8, No. 9, pp.356–363.